RESEARCH ARTICLE

Quantum Spin Hall Insulator State in HgTe Quantum Wells

Markus König[1], Steffen Wiedmann[1], Christoph Brüne[1], Andreas Roth[1], Hartmut Buhmann[1], Laurens W. Molenkamp[1,*], Xiao-Liang Qi[2], Shou-Cheng Zhang[2]

[1] *Physikalisches Institut (EP III), Universität Würzburg, D-97074 Würzburg, Germany.*

[2] *Department of Physics, McCullough Building, Stanford University, Stanford, CA 94305–4045, USA.*

* To whom correspondence should be addressed. E-mail: molenkmp@physik.uni-wuerzburg.de

– Hide authors and affiliations

Science 02 Nov 2007:
Vol. 318, Issue 5851, pp. 766-770
DOI: 10.1126/science.1148047

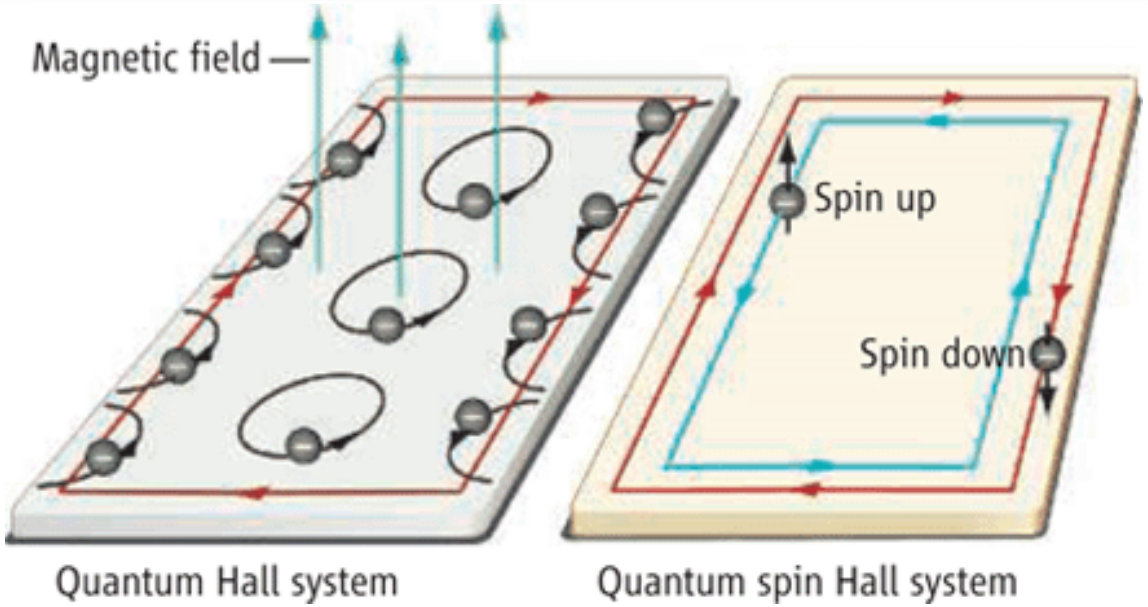

REPORT

Quantum Spin Hall Effect and Topological Phase Transition in HgTe Quantum Wells

B. Andrei Bernevig[1,2], Taylor L. Hughes[1], Shou-Cheng Zhang[1,*]

[1] *Department of Physics, Stanford University, Stanford, CA 94305, USA.*

[2] *Kavli Institute for Theoretical Physics, University of California, Santa Barbara, CA 93106, USA.*

* To whom correspondence should be addressed. E-mail: sczhang@stanford.edu

– Hide authors and affiliations

Science 15 Dec 2006:
Vol. 314, Issue 5806, pp. 1757-1761
DOI: 10.1126/science.1133734

Theory – QSH and Topological Phase Transition

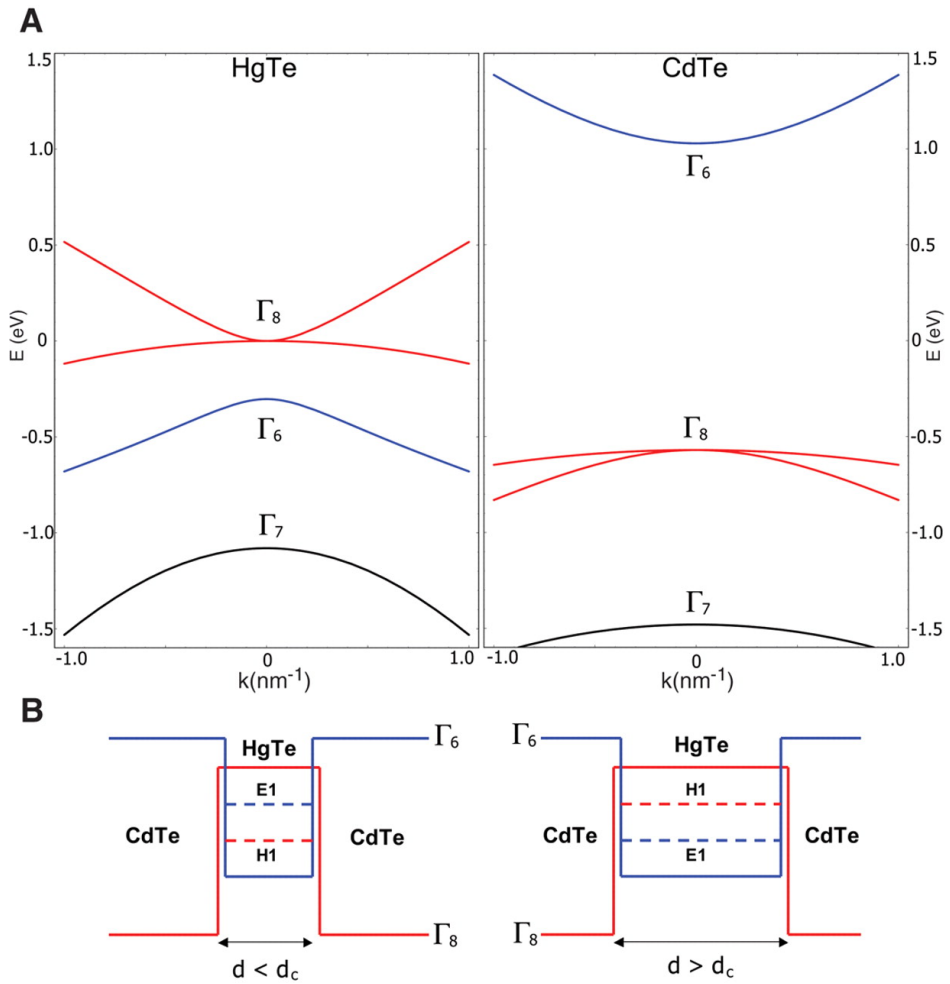

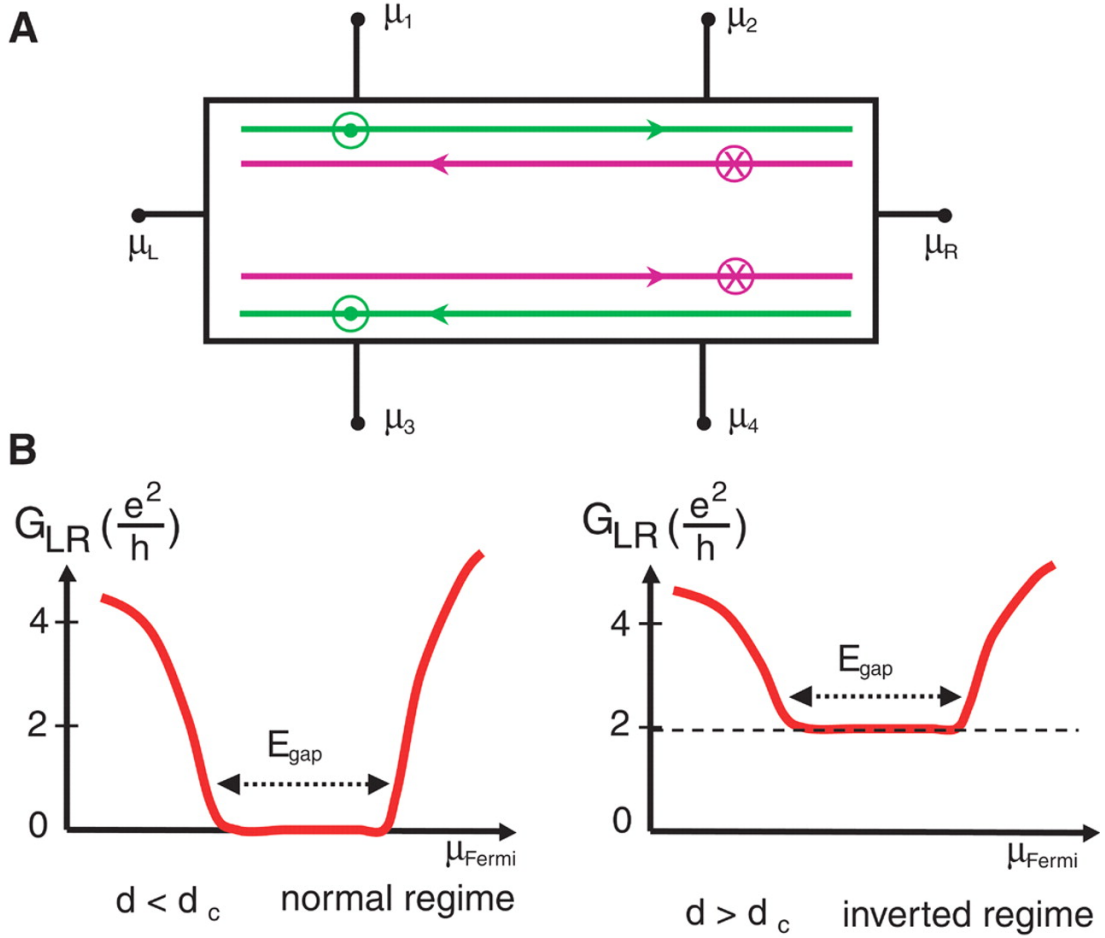

HgTe 2DEG

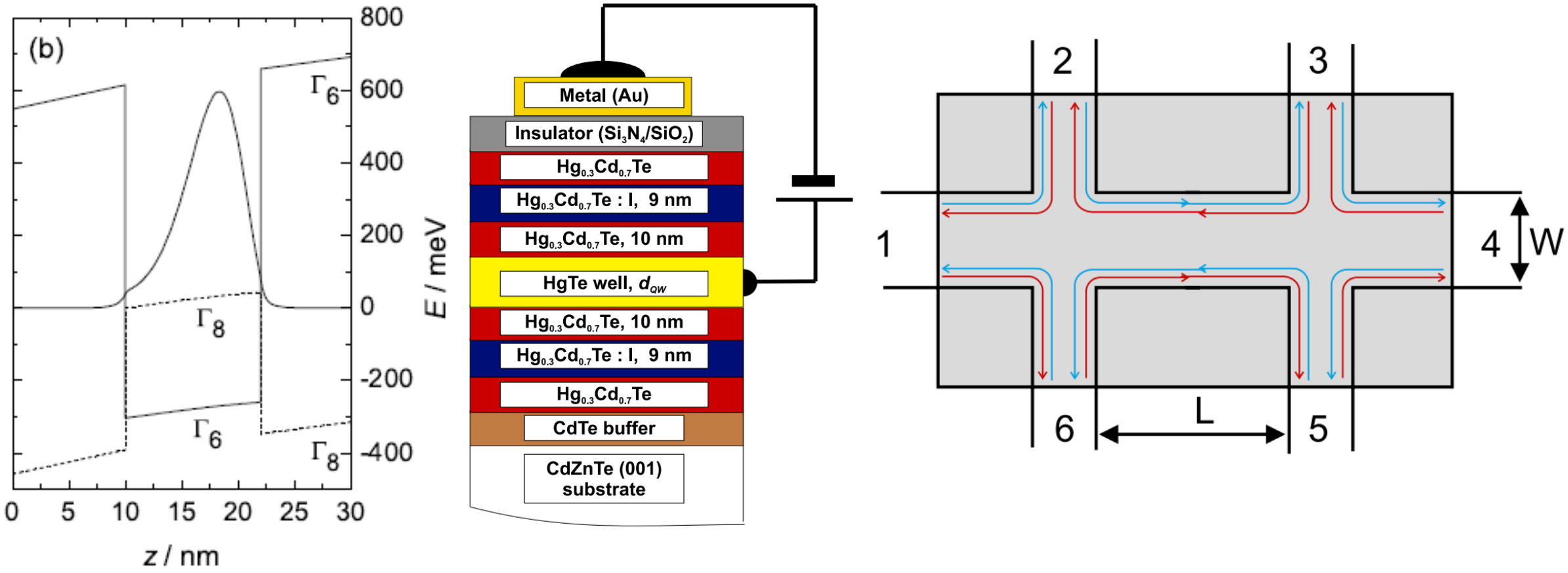
(b)
Γ6
Γ8
Γ6
Γ8
800
600
400
200
0
-200
-400
0
5
10
15
20
25
30
z / nm
E / meV
Metal (Au)
Insulator (Si3N4/SiO2)
Hg0.3Cd0.7Te
Hg0.3Cd0.7Te : I, 9 nm
Hg0.3Cd0.7Te, 10 nm
HgTe well, dQW
Hg0.3Cd0.7Te, 10 nm
Hg0.3Cd0.7Te : I, 9 nm
Hg0.3Cd0.7Te
CdTe buffer
CdZnTe (001) substrate
1
2
3
4
5
6
W
L

Quantum Hall Effect

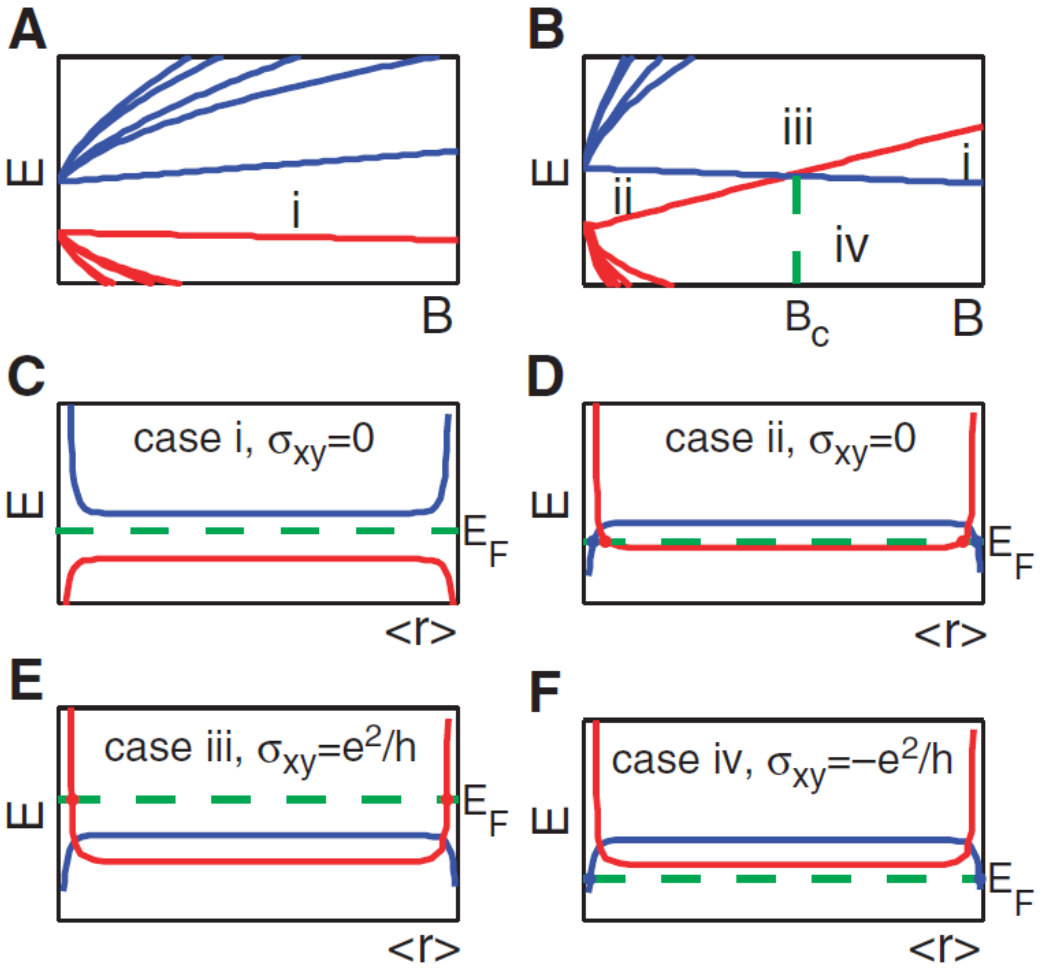

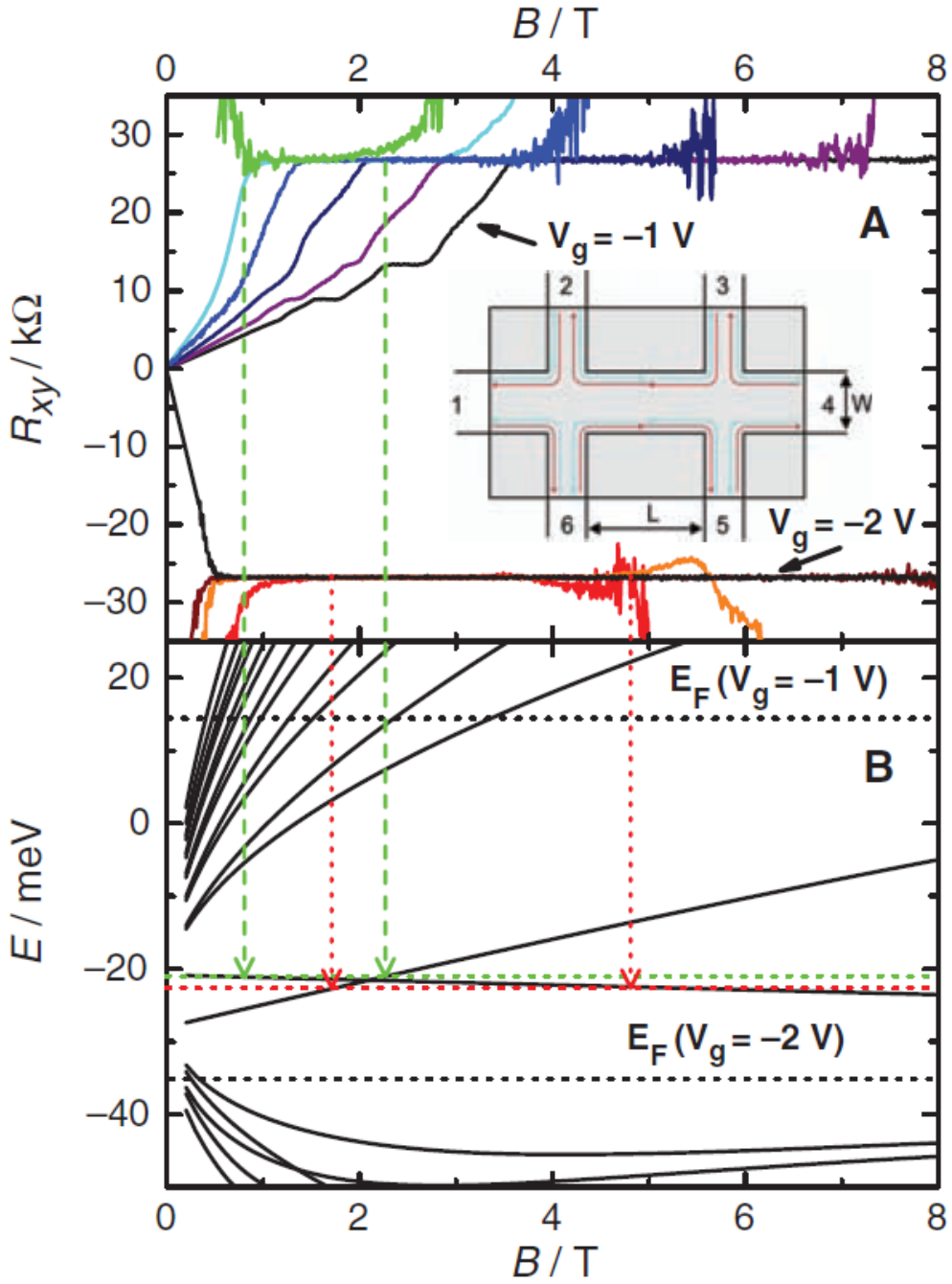

Topological Phase Transition

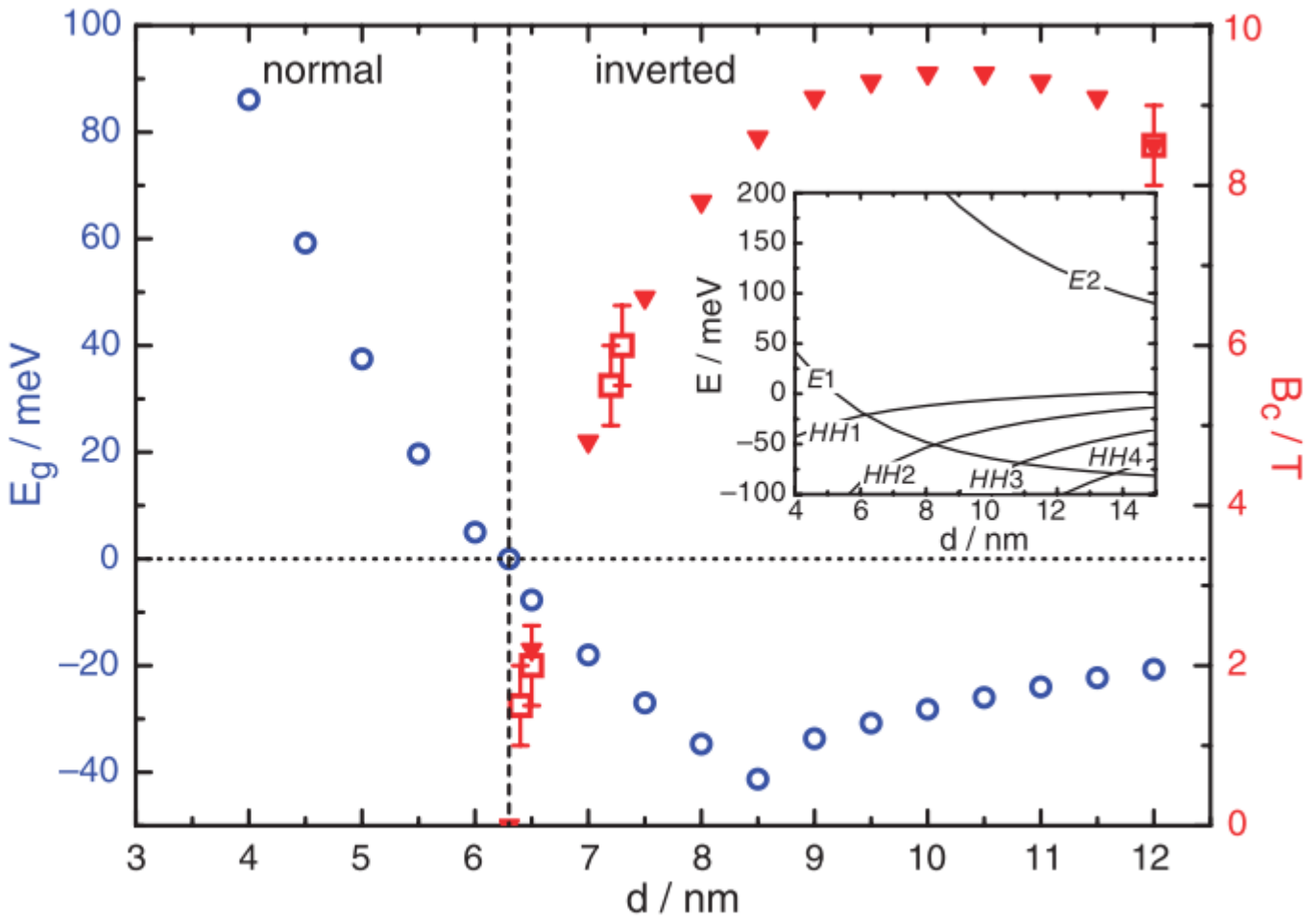

Fig. 3. Crossing field, $B^c_\perp$ (red triangles), and energy gap, E_g (blue open dots), as a function of QW width d resulting from an eight-band **k·p** calculation. For well widths larger than 6.3 nm, the QW is inverted and a mid-gap crossing of Landau levels deriving from the *HH*1 conductance and *E*1 valence band occurs at finite magnetic fields. The experimentally observed crossing points are indicated by open red squares. The inset shows the energetic ordering of the QW subband structure as a function of QW width d. [See also (*17*)].

Helical edge mode – Topologically protected

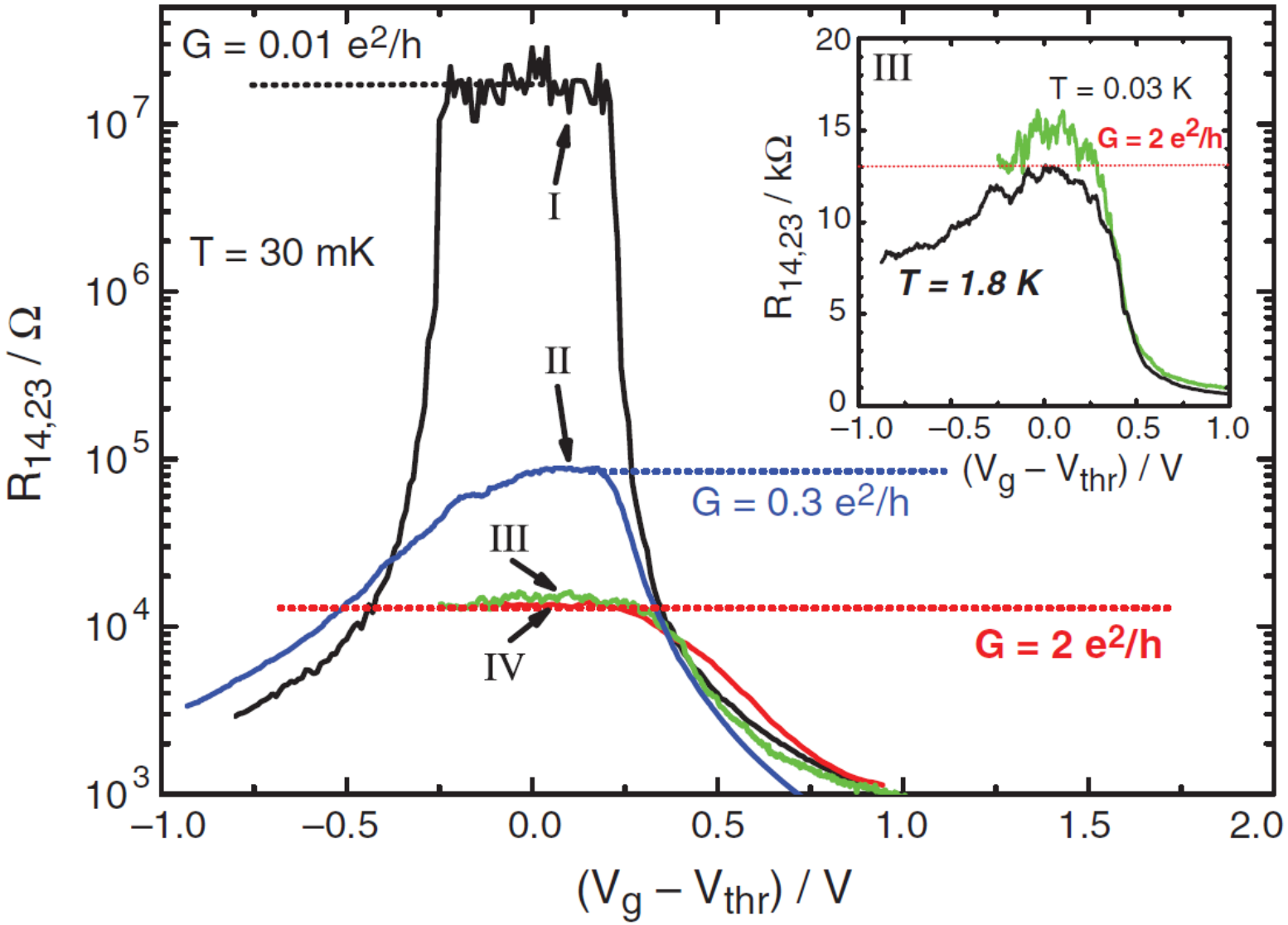

Fig. 4. The longitudinal four-terminal resistance, $R_{14,23}$, of various normal (d = 5.5 nm) (I) and inverted (d = 7.3 nm) (II, III, and IV) QW structures as a function of the gate voltage measured for B = 0 T at T = 30 mK. The device sizes are (20.0 × 13.3) μm² for devices I and II, (1.0 × 1.0) μm² for device III, and (1.0 × 0.5) μm² for device IV. The inset shows $R_{14,23}(V_g)$ of two samples from the same wafer, having the same device size (III) at 30 mK (green) and 1.8 K (black) on a linear scale.

Magneto-conductance – TR Breaking

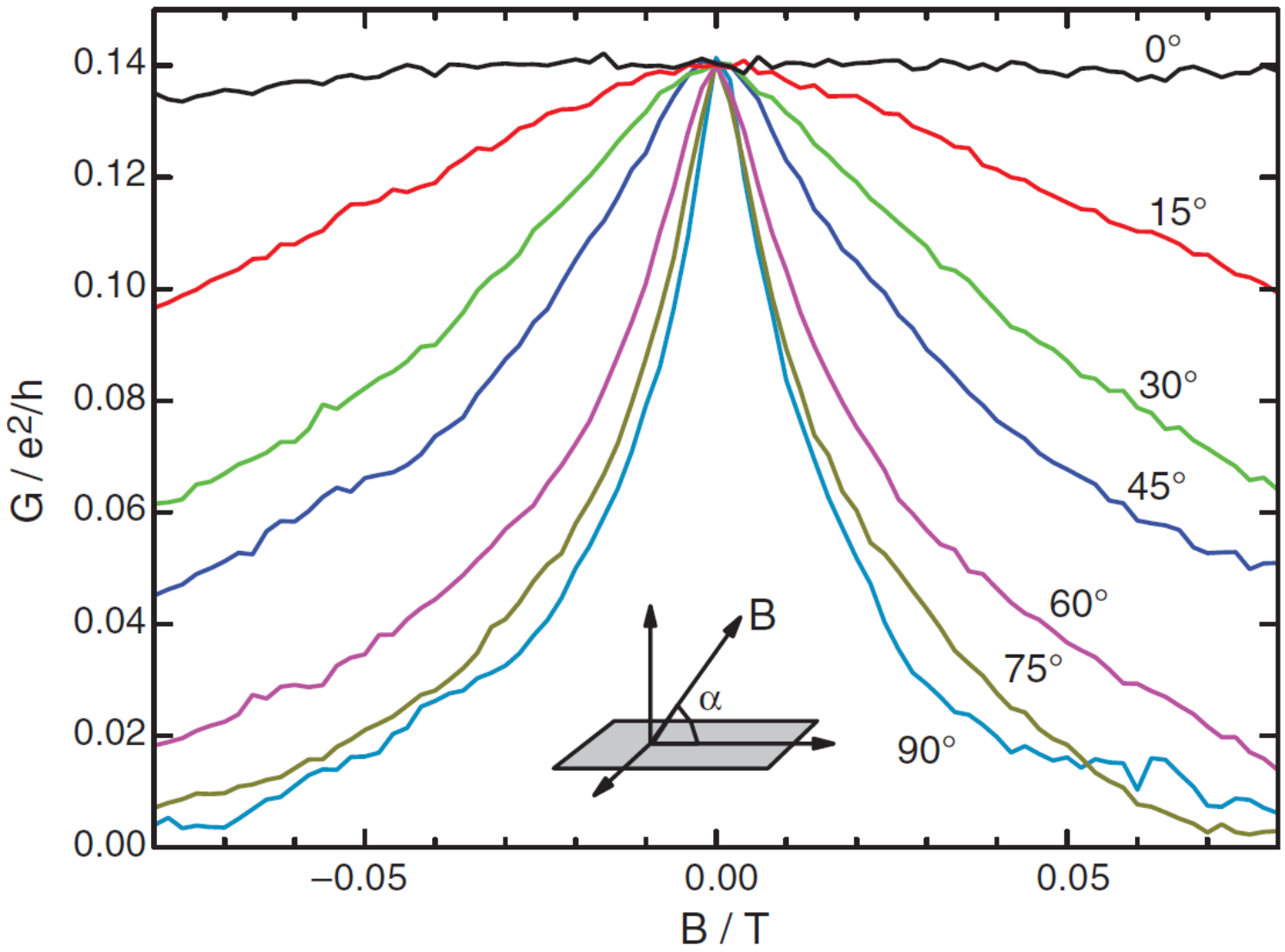

Fig. 5. Four-terminal magnetoconductance, $G_{14,23}$, in the QSH regime as a function of tilt angle between the plane of the 2DEG and applied magnetic field for a d = 7.3-nm QW structure with dimensions ($L \times \Omega$) = (20 × 13.3) μm^2 measured in a vector field cryostat at 1.4 K.